

Cinder cones of Mount Slamet, Central Java, Indonesia

IGAN S. SUTAWIDJAJA¹ AND R. SUKHYAR²

¹Pusat Vulkanologi dan Mitigasi Bencana Geologi, Badan Geologi, Jl. Diponegoro No. 57 Bandung

²Badan Geologi, Jl. Diponegoro No. 57 Bandung

ABSTRACT

The Mount Slamet volcanic field in Central Java, Indonesia, contains thirty five cinder cones within an area of 90 sq. km in the east flank of the volcano. The cinder cones occur singly or in small groups, with diameter of the base ranges from 130 - 750 m and the height is around 250 m. Within the volcanic field, the cinder cones are spread over the volcanic area at the distance of 4 to 14 km from the eruption center of the Slamet Volcano. They are concentrated within latitudes 7°11'00" - 7°16'00" S, and longitudes 109°15'00" - 109°18'00" E. The density of the cinder cones is about 1.5 cones/km².

Most of the cinder cones lie on the Tertiary sedimentary rocks along the NW-trending fault system and on radial fractures. The structural pattern may be related to the radial faults in this region. The cone surfaces are commonly blanketed by Slamet air-falls and lava flows.

The deposits consist of poorly bedded, very coarse-grained, occasionally overlain by oxidized scoria, and large-sized of ballistic bombs and blocks. There are various kind of volcanic bombs originating from scoriae ballistic rock fragments. The other kind of volcanic bombs are breadcrust bomb, almond seed or contorted shape.

All of the cinder cones have undergone degradation, which can be observed from the characters of gully density and surface morphology. By using Porter parameters, Hco is equal to 0.25 Wco, whilst Wcr is equal to 0.40 Wco. The Hco/Wco ratio is higher than Hco = 0.2 Wco reference line. A radiometric dating using K-Ar method carried out on a scoria bomb yields the age of 0.042 ± 0.020 Ma.

Keywords: Cinder cone, scoriae, ballistic bombs, air-fall, lava flow, radiometric dating.

SARI

Daerah vulkanik Gunung Api Slamet di Jawa Tengah, Indonesia, mempunyai tiga puluh lima kerucut sinder dalam area 90 km² di lereng timur gunung api ini. Kerucut sinder hadir baik secara tunggal maupun dalam kelompok kecil dengan garis tengah alasnya berkisar antara 130 - 750 m dengan nilai rata-rata 430 m, dan tingginya mencapai 250 m. Dalam area vulkanik ini, kerucut sinder tersebar pada radius 4 - 14 km dari kawah Gunung Slamet, dan terhimpun di antara Lintang 7°11' - 7°16'S dan Bujur 109°15' - 109°18'T. Kerapatan kerucut sinder ini adalah 1,5 kerucut/km².

Sebagian besar kerucut sinder ini muncul pada batuan sedimen Tersier sepanjang sistem sesar mengarah barat laut - tenggara, dan pada rekahan radial. Di daerah ini, pola struktur kemungkinan berhubungan dengan rekahan radial tersebut. Bagian permukaan kerucut sinder pada umumnya tertutup endapan jatuhnya piroklastika dan aliran lava Gunung Slamet. Endapannya terdiri atas skoria berukuran kasar sampai bom balistik, tidak berlapis, dan permukaan butirannya kadang-kadang teroksidasi, terutama pada butiran bom atau bongkah. Jenis bom tersebut umumnya berasal dari bom skoria balistik. Jenis lain di antaranya bom kerak-roti, bentuk biji almon, atau bentuk terpilih.

Semua kerucut sinder mengalami degradasi akibat torehan pada lerengnya dan perubahan morfologi permukaannya. Dengan menggunakan parameter Porter diperoleh Hco sebanding dengan 0,25 Wco, sedangkan Wcr sebanding dengan 0,40 Wco. Rasio antara Hco/Wco lebih besar dari Hco = 0,2 Wco garis acuan. Pentarikan umur bom skoria dari salah satu kerucut sinder dengan metode radiometrik K-Ar menunjukkan umur 0,042 ± 0,020 jtl.

Kunci: Kerucut sinder, skoria, bom balistik, jatuhnya piroklastik, aliran lava, pentarikan radiometrik.

INTRODUCTION

Mount Slamet is situated near the boundary between West and Central Java Provinces about 22 km northwest of Purbalingga, Central Java. The highest peak is about 3428 m above sea level, and geographically it is located at 7°14'30" S and 109°13'00" E. The study area is situated in the eastern slope of Mount Slamet and is bounded by latitudes 7°10'00" to 7°17'00" S, and longitudes 109°12'00" to 109°22'00" E (Figure 1). The study area comprises 242 square kilometers of which the major part consists of steep slopes. The study area is accessible from three major towns, namely Purbalingga, Pemalang and Tegal, of which Moga Village at Pemalang is the main access to the study area.

This paper is part of a geologic mapping carried out in 1990 and was revised in 2006. The 2006 study was focused on the thirty five cinder cones located in the east flank of Mount Slamet that covers an area of about 90 km². A base map of 1: 50 000 in scale used in the field was compiled from aerial photographs with the scaled of 8 inches equal 1 mile, provided by Volcanological Survey of Indonesia. The thirty five cinder cones show variation in shape, base of the

cone width, height, and crater diameter. Most of the cones have been eroded as shown by evidences of incipient broad shallow radial gullies, and the crater openings occurring to any directions.

The cinder cones are formed due to the Strombolian eruption. The cone-building process is mainly one of ballistic deposition and slumping, with some of the fine-grained airfall carried away by wind (McGetchin *et al.*, 1974). Macdonald (1972) defines cinder cones as small truncated, cone shaped volcanic hills with the top contains bowl-shaped craters. The hills, often called tephra cones or scoria cones, are built up by an accumulation of cinders and other pyroclastic debris around approximately circular vent. The cinder cones are primarily constructed by moderately explosive eruptions, pristine cone morphometry depending principally upon explosive eruptions that are based on pyroclastic size, distribution, ejection velocity, and ejection angle (Settle, 1979).

GEOLOGIC SETTING

General Geology

The morphology and geologic investigations of Mount Slamet and its vicinity have been carried out by Neumann van Padang (1951), Pardyanto (1971), Djuri (1975), and finally by Sutawidjaja *et al.* (1985). Mount Slamet lies on the western part of the North Serayu Range and belongs to the Bogor Zone (Van Bemmelen, 1949). Pardyanto (1971) suggested that Mount Cowet (Old Slamet Volcano) was built in mid- Quaternary, and had erupted lava and pyroclastic materials. In addition, Hamilton (1979) stated that the Late Cenozoic volcanoes rise mostly above Neogene marine strata, rather than outcropping in pre-Tertiary complexes. Furthermore the young volcanic rocks in Java are markedly more mafic in average composition than those of Sumatera.

Sedimentary rocks of both Tertiary and Quaternary age are exposed in the study area. Most of the Tertiary deposits are concealed beneath the Quaternary volcanic products of Mount Slamet, which ranges from a thin layer to a cover more than 2000 m thick. Van Bemmelen (1949) divided Mount Slamet products into two major volcanic types: 1) Volcanic I, which was produced by the Old Slamet Volcano,

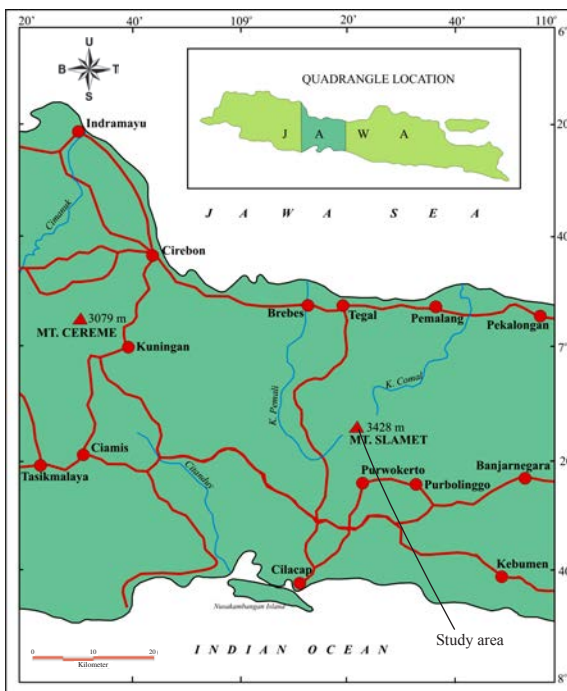


Figure 1. Index map showing location of the Mount Slamet and cinder cones area, Pemalang and Purbalingga Regencies, Central Java, Indonesia.

as Pardyanto (1971) considered that the Old Slamet products were erupted from Mount Cowet, lying in the western part of Mount Slamet, and 2) Volcanic II products being the result of Mount Slamet eruptions (Figure 2). Sutawidjaja *et al.* (1985) stated that the Old Slamet rocks consist of hornblende and pyroxene andesites and eruptive materials from Mount Slamet, characterized by andesitic and olivine basalts.

STRUCTURAL SETTING

General Feature

The cinder cone complex of Mount Slamet is located close to the Banyumas depression, equivalent to the Banyumas Fault Zone (Tjia, 1978). Physiographically, it is included to the western part of the North Serayu Range and the eastward continuation of the Bogor Zone (Van Bemmelen, 1949). The main tectonic features of the Quaternary tectonism are associated with the occurrence of island arc structures and negative isostatic gravity anomalies (Katili, 1969).

The tectonism activity, which for at least at the eastern zones of the area, was partly pre-volcanic

event, had caused the tilting and folding of the Miocene and Pliocene sedimentary substratum. The tectonic elements which considerably affect the volcanic rock, especially Old Slamet volcanic rocks are normal fault system to which the activity of Mount Slamet is presumably connected. This fault system with a gravity slip component has controlled several flank eruptions of lava flow in the west foot of Mount Slamet, whereas in the mapped area, the subsided blocks or footwalls are commonly filled by lava flows.

Structural Control of the Area

The area of Mount Slamet is occupied by radial strike slip faults associated with the formation of Mount Slamet and the cinder cones (Figure 3). The cinder cone field is situated in an area of extensive faulting and is associated with lava flows from the main crater of Mount Slamet. There are two main directions of faulting: northeast - southwest and northwest - southeast (Djuri, 1975). Both sets of faults are strike slip left-lateral oblique slip faults. Several grabens and normal faults are mainly associated with Slamet volcanic deposits, particularly the Old Slamet or Mount Cowet (Sutawidjaja, 1985). On the east slope of Mount Slamet, both types of

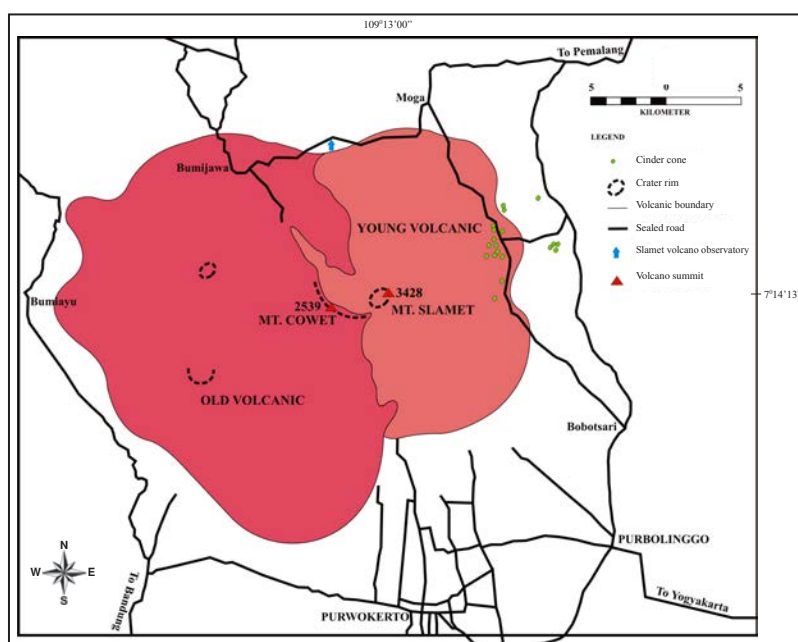


Figure 2. Map showing the distribution of Old Slamet (andesitic and rhyolitic) and Young Slamet (basaltic andesite) rocks. The investigated cinder cones lie on the east slope of Mount Slamet.

faults, in particular those trending northwest and northeast, control the alignment of volcanic vents of the cinder cones. In the eastern part of the area, the relationship between tectonic stress and cinder cone lineaments is more obvious. The area surrounding the summit of Mount Slamet is characterized by east - west fractures and parallel lineaments of the cinder cones. These fractures may be related to the east - west-trending normal faults just east and west of the volcanic field. The characteristic fault pattern is believed to be a result of crustal contraction of South Java subduction zone (Katili, 1969).

The cinder cones of Mount Slamet, which mostly lie along the northwest-trending fault system are also controlled by radial normal faults. The most evident dislocation is the northwest strike-slip fault that cuts the Tertiary rock formations down throwing them to the west and offsetting the Halang Formation by hundreds of meters. Concentric lineaments surrounding the central volcano are possibly defined by the arrangement of the cinder cones. There are at least five concentric lineaments, which may be ring fractures (Figure 3). They have spacings of 1 to 4 km. A system of radial fractures which is approximately centered on the vent of Mount Slamet, is also evidenced in the formation of the cinder cones. These fractures mostly displace the Tertiary rock formations, some

of them can be traced on the Quaternary volcanic rocks by a northward subsidence and tilt of faulted blocks. The intrusion of diorite also occurs along one of those faults, indicated by the emplacement of an east - west elongated dome.

The most important structure which presumably displaces rocks of the Old Slamet volcanic body is a northeast fracture (probably normal fault). It is a large collapse structure towards north followed by multiphase eruptions to build up the young cone, as Mount Slamet. There is a possibility that the collapse was accompanied by a formation of the cinder cones. The collapse probably pushed up the northeast part of the Tertiary rocks and formed concentric gentle folds (Figure 4). The structural framework of the area which includes the general pattern of radial fractures is centered on the vent of Mount Slamet. The cinder cone distribution pattern is controlled by near surface fracture systems. Within the Slamet cinder cone field, rising magma encountered multiple sets of crustal fractures and tends to be funnelled into fracture intersections to produce an overall scattered pattern of cone distribution. In contrast, magma rose within the central conduit of a volcano and scattered through the fracture zone within the Tertiary rock formations to form magma pockets. The cinder cones were formed by high gas

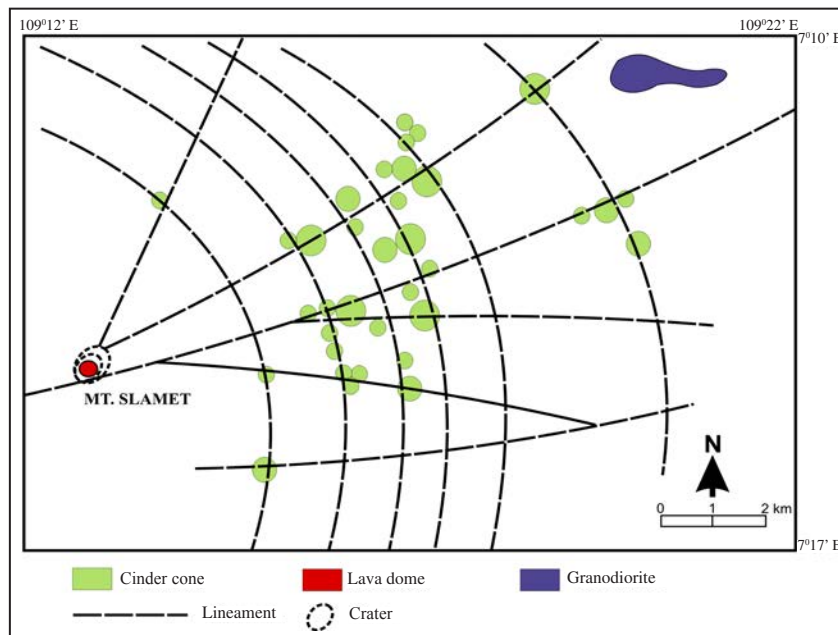


Figure 3. Fractures and concentric lineaments, probably control the cinder cone formation.

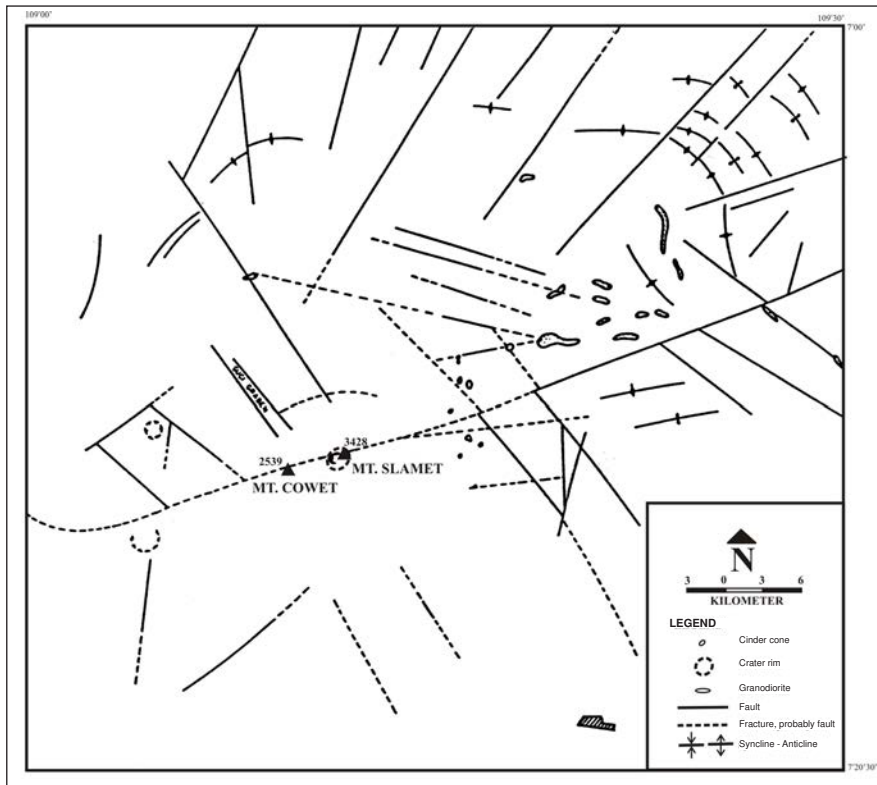


Figure 4. Geological structures of the mapped area, compiled mainly from Djuri (1975) and Sutawidjaja (1985), with some addition to the structures/fractures.

basaltic eruptions from the magma pockets which are controlled by surface fracture systems (Sudradjat, oral communication, 2006). Settle (1979) stated that magma rising within the central conduit of a volcano is more likely to be shunted into one of the major fracture zones within the volcano's edifice and discharged somewhere along the surface expression of the fracture. Generally, it produces a preferentially aligned pattern of cone distribution with individual cones concentrated in specific radial sectors on the flanks of the volcano. Settle (1979) also described the relatively smaller average size and spacing of cinder cones formed upon the flanks of volcanoes. This may reflect the relative ease with which the eruptive activity can shift to higher or lower elevations along a continuous fracture zone in response to variations in magmatic pressure during periods of active eruption. Fracture zones exposed upon the flanks of volcanoes commonly extend over a wide range of elevation, encompassing several kilometers of vertical topographic relief (Mac Donald, 1972).

GEOMETRY OF THE CINDER CONES

Morphology

Cinder cone is the most common volcanic landform created by a Strombolian activity and the cone-building process is one of the ballistic deposition and slumping, with some of the finer-grained airfall carried away by the wind (McGetchin *et al.*, 1974; Heiken, 1978). Cinder cones on Mount Slamet range from small mounds less than 100 m in basal diameter and only several meters high, to hills as much as 750 m across at the base and 250 m high. The majority, however, are 250 to 600 m wide and 30 to 150 m high. Differences in size and gross morphology among cones largely reflect variations in magnitude and duration of eruption (Porter, 1972). The cinder cones occur singly or in small groups, apparently at random about the east slope of the volcano (Figure 5 and 6).

The cinder cone craters generally broaden and deepen, as eruption progresses, leading to a col-

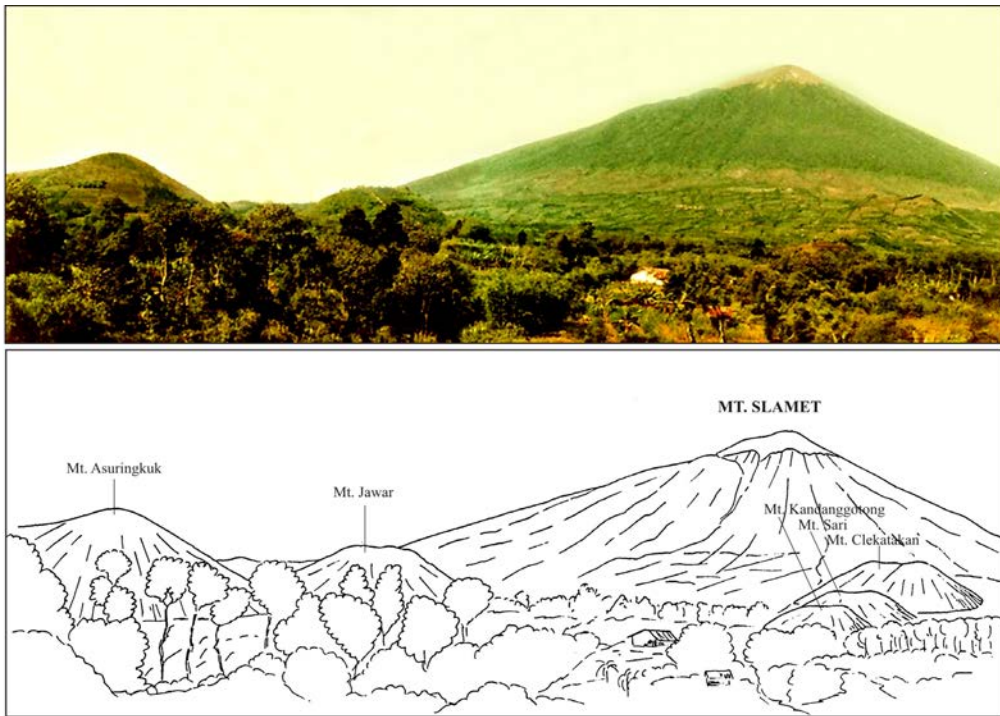


Figure 5. Distribution of cinder cones on the east flank of Mount Slamet, showing several cinder cones, viewed to the western area.

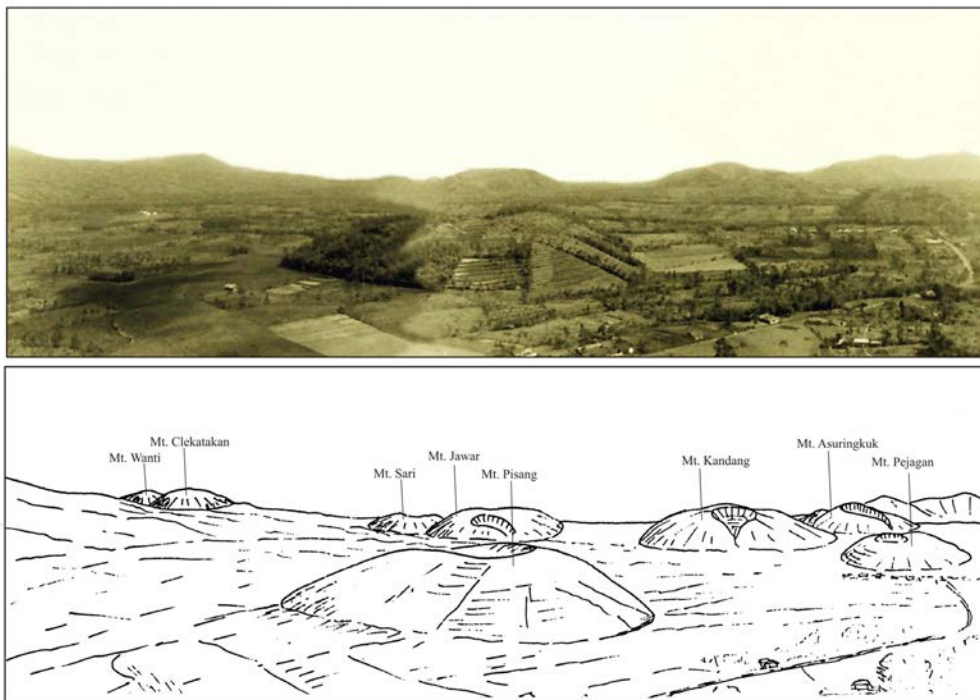


Figure 6. Distribution of cinder cones on the east flank of Mount Slamet and cinder cone flatland, seen from Mount Lompong towards north.

lapse and slump structure inside their topographic rims (Wohletz and Sheridan, 1983). Some of the cinder cones have more than one crater that could be caused by changing the vent location during an eruption, and craters opening in particular directions are commonly found (Figure 7).

Lava flows from Mount Slamet associated with cinder cones were commonly produced by Mount Slamet's vent and flank eruptions. The former lava flows generally flowed down around the flanks, enclosing and partially burying the cinder cones. Most of the cinder cones lie on the Tertiary sediments, and are buried by Mount Slamet volcanic products, particularly lava flows and pyroclastic airfalls. Almost all of the cinder cones are covered by the Slamet pyroclastic airfall, ranging from 50 cm to 2 m in thickness. Most of the cones show asymmetric rims, with one quadrant of the rim standing higher than adjacent quadrants. In many instances the opposing quadrant also stands higher than the intervening quadrants, producing a bi-peaked rim (Figure 7). Such an asymmetric rim was the result of strong near-surface wind during eruptions which drift ejecta leeward or, alternatively, to clogging of the vent, which can direct a shower of pyroclastic fragments in a specific direction (Porter, 1972). Porter concluded that the most asymmetrical cones appear to result from persistent wind action, for the highest rim of the cone invariably lies on the same side as the tephra plume that was deposited downwind.

Generally the cinder cones have experienced some erosion to show evidence of incipient gully in the form of broad shallow radial swales. Some of the cones show a modified surface with strong erosion in a specific direction, so that the opening crater (Figure 7) by encroachment of heavy rainfalls. Verwoerd and Chevallier (1987) classified the types of volcanic cones based on monogenetic explosive volcanic phenomena (energy, landforms, deposits) in relation to the water/magma ratio, and he analyzed that cinder cones were built by ballistic subaerial magmatic eruptions, and cinder cones with or without lava flows, often seem to occupy the same site as an earlier tuff cone.

Erosive processes operating upon a cone field may vary significantly as the regional weathering environment changes over geological time scales.

For example, weathered deposits on the flanks may be exposed to a variety of weathering environments ranging from tropical conditions near the base of the volcano to subarctic conditions near the summit (Porter, 1972). In addition, Scott and Trask (1971) suggested that since the ratio of cone surface area to cone volume decreases with increasing cone diameter, fluvial processes may erode smaller cinder cones at relatively faster rates.

Distribution

A total of thirty five cinder cones in Mount Slamet were identified from topographic maps and aerial photographs, scale 1: 50,000 in conjunction with field observations. The majority of the cinder cones are concentrated between latitudes 7°11'00" to 7°16'00" S, and longitudes 109°15'00" to 109°18'00" E (Figure 7). The nearest cone is 4 km and the farthest one is 14 km from the vent of Mount Slamet. A local concentration of the cinder cones is at 14 km from the vent, where locally the cone density is 1.5 cones/km². Those on the east side of Mount Slamet delineate rather strikingly the principal fault zones, which are indicated by lineaments particularly in the Tertiary rock formations. The northwest strike slip faults controlled several groups of the cones. In addition to these pronounce sub linear groupings the cinder cones are arranged in actuate patterns suggestive of concentric fracture zones (see Figure 3).

The cinder cones occur singly or in small groups, apparently at random around the east slope of the volcano. Some, possibly, are aligned and represent a second-order fracture system which has a radial pattern and is centered at the volcano. In general, the cinder cone distribution is associated with a fracture system particularly with northwest strike slip faults. The most dense concentration occurs between elevation of 1100 and 1500 m above sea level. A small cluster occurs between elevation of 800 and 900 m above sea level. Almost all of the identifiable cones are wholly or partially buried by younger Slamet pyroclastic airfalls and lava flows. In this paper the distribution of Slamet airfall over the cinder cones and the Tertiary rock units was not plotted. The cone formation occurred along the northwest strike slip faults, in the form of fracture zones that were penetrated by magma to form cinder cone.

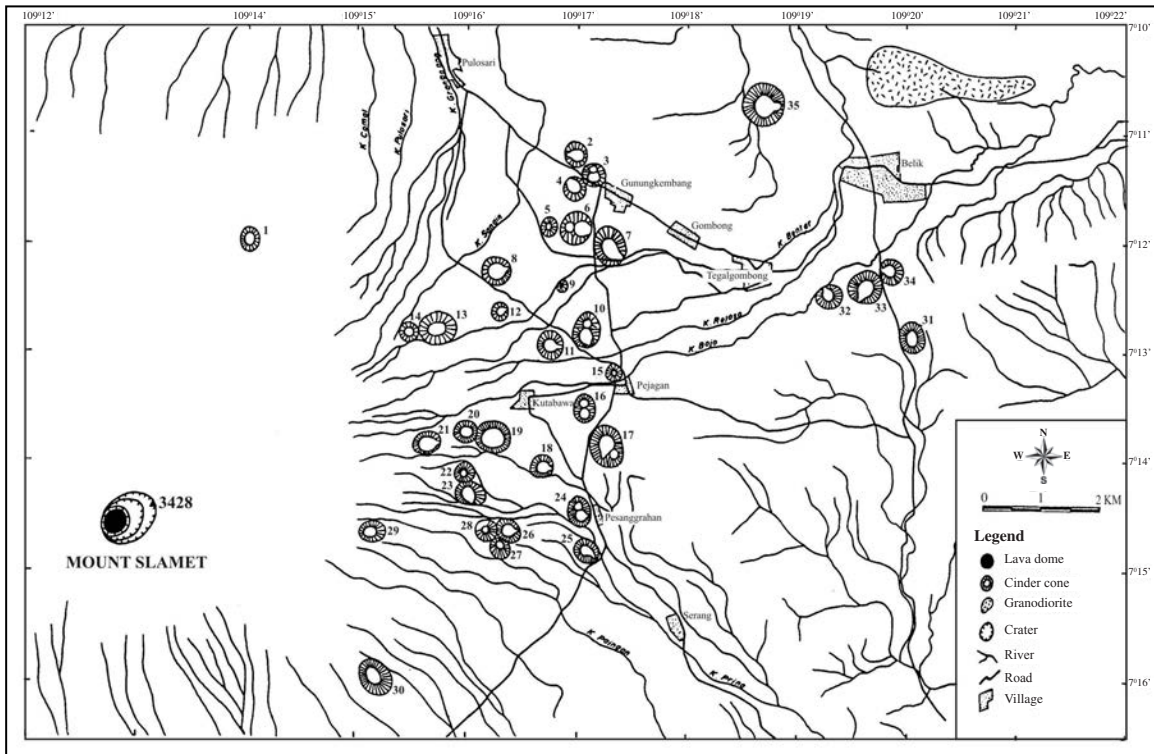


Figure 7. The distribution of the cinder cones in the east flank of Mount Slamet. Number of the cone corresponds to the Table 1.

Major structural lineaments exposed along the flank of the volcanoes are interpreted as the surface expressions of fracture zones that penetrate a volcano's edifice and commonly extend to the central magma conduit at the core of a volcano (Nakamura, 1977). Settle (1979) observed that in the course of subsequent explosive activity, magma may be funneled into a variety of fracture intersections, or it may be locally injected into regional fractures at depth, accounting for the local alignment of small groupings of cones.

Morphometric Analyses

Cinder cones show various stages of degradation, which can be estimated from relative ages. Wood (1980) examined the processes of cone modification for the two most important degradation mechanisms : (1) burial of the cone flanks by subsequent lava flows, and (2) erosion and mass wasting of material from the cone flanks. Kear (1957) devised four stages in the erosion of large volcanic cones (composite volcanoes) in New Zealand, where the connections between age and degree of erosion

expressed present cone shape. In this case the dimensions of cinder cones are systematically measured, using the terminology of Porter (1972), with W_{co} = cone basal diameter, W_{cr} = crater diameter, H_{co} = cone height; and α = cone slope angle (Figure 8). Some cones are less than the contour interval of maps used for measurement; therefore, the depth of the crater is not used as a descriptive parameter.

Height/width ratios of Mount Slamet cinder cones

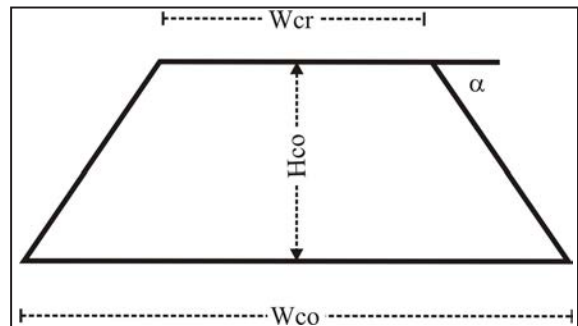


Figure 8. Schematic diagram illustrating the parameters used to estimate cinder cone size (after Porter, 1972).

show a little variation, the cone height commonly being 0.25 of the cone basal width (Figure 9b). Crater dimensions are also a function of cone size, with crater width typically being 0.40 of the basal diameter of the cone (Figure 9a). The ratio of the cone height to the difference between basal width and crater width averages 0.40 which is equivalent to a mean slope of 28° for the flanks of the cinder cone. That value is approximately an equilibrium angle of repose for tephra comprising the cinder cones on the volcano (Porter, 1972). Measured maximum slope angles were remarkably consistent around a given field, as well as among cones of different ages, and typically will fall within the range of 27° to 29° .

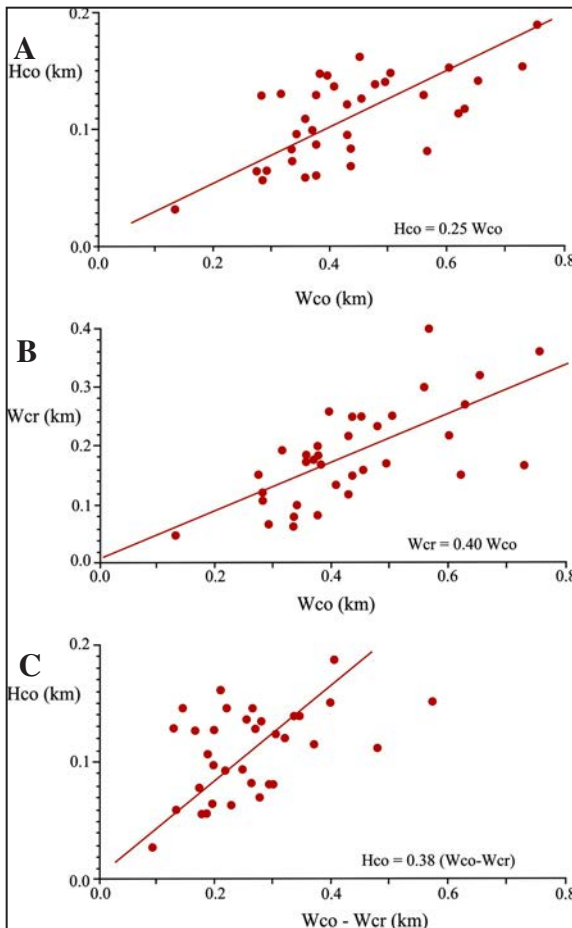


Figure 9. Morphological characteristics of cinder cones on Mount Slamet; (a) the height commonly being 0.25 of the basal width, (b) crater width typically being 0.40 of the basal diameter, (c) ratio of cone height to the crater and basal diameter.

The circumferences of crater rims and cone bases were determined where the generally equidistant topographic contours abruptly widen. Although the crater was not visible on the topographic maps, the diameter of the craters could be determined from the high quality aerial photographs.

Cone basal diameter is defined here as the average (mean) of the maximum and minimum base diameter measured for each cone. The location of a cone basal edge was determined in two ways: explicitly from aerial photographs and direct interpretation of the point of topographic inflection along a cone exterior surface by defining an abrupt change in the spacing and/or circularity of topographic contours outlining the cone.

Cone height is defined here as the difference between the average basal elevation and the maximum elevation which is observed at the cone rim crest or summit. Crater width for each cone was easily obtained from aerial photographs, even where each cone crater shows various widths and shapes, many of them do not have circular crater. Cone separation distance is reported here as the horizontal distance between a cinder cone and its nearest neighbour and is measured between the centers of two cones.

Porter (1972) has previously reported an empirical relationship between cone height (Hco) and cone basal diameter (Wco) in which cone height $(Hco) = 0.18 Wco$ based upon a select group of thirty Mauna Kea cinder cones that are presumably characterized by a fresh morphological appearance (Figure 10). Bloomfield *et al.* (1977) has examined the morphometry of forty one cinder cones within a section of the Mexican Volcanic Belt to the east of Paricutin. He reported a mean Hco/Wco ratio for Holocene cones of 0.21 and a mean ratio of Hco/Wco of 0.19 for relatively young "well-formed" Pleistocene cones. Therefore the $Hco = 0.2 Wco$ reference line shown in Figure 12, may characterize the initial shape of cinder cones formed in both types of volcanic provinces prior to the erosive degradation.

The most common erosive processes on the cinder cones occur within the craters. The materials from crater walls were eroded and carried by rain fall through the opened crater. Furthermore, expansions of the craters were indicated by high Wcr/Wco ratios, which may be specific to the cinder cones at Mount Slamet.

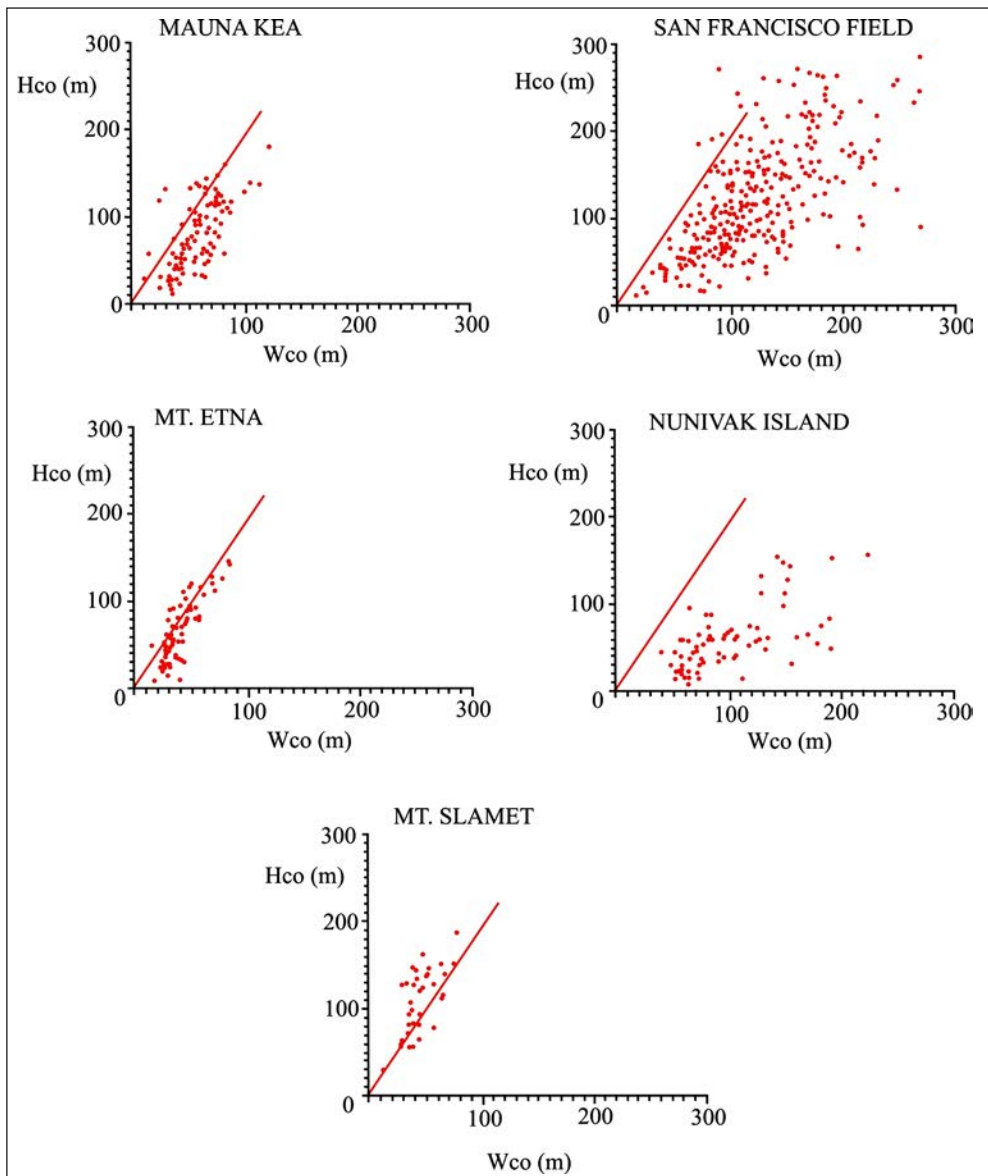


Figure 10. Comparison of the shape of cinder cones between Mount Slamet cinder cone and data from Settle (1979). Cinder cone height (Hco) is graphed versus cone basal diameter. The straight line in each graph represents the relationship of $Hco = 0.2 Wco$ which may describe the average initial shape of cinder cones prior to erosive degradation.

Morphometric Analyses

A radiometric dating has been obtained from one sample using the K-Ar method. A whole rock date from the basalt scoria bomb of Gunung Dipajaya cinder cone yields 0.042 ± 0.020 Ma. This age is expected to represent all of the cinder cones, because they have similar character, such as degradation stages, morphometric parameters, and rock conditions

Volume of Cinder Cones

Morphometric parameters of cinder cone were obtained from 1:50,000 topographic maps and aerial photographs. These parameters include cone height (Hco), cone basal diameter (Wco), and crater diameter (Wcr) (see Figure 8). Most of the cinder cones show a symmetrical truncated cone shape, but cinder cones that erupted on an inclined basement surface were often breached or elongated. To allow for this,

W_{co} and W_{cr} are defined as the arithmetic means of the maximum and minimum values of the cone crater widths. H_{co} is the elevation difference between the summit of the cinder cone and its base. Calculation of the cone basal and crater diameters, and cone height are presented in Table 1. From these values, the volume of the cinder cones could be calculated using Torarinsson formula (1981) below.

$$V_{co} = \pi H/12 \cdot (W_{cr}^2 + W_{cr}W_{co} + W_{co}^2)$$

Where :

V_{co} = volume of cinder cone (in lan^3)

H = cone height (in km)

W_{cr} = crater diameter (in lan)

W_{co} = cone basal diameter (km)

The cinder cones are often partly buried by lava flows from Mount Slamet, and almost the whole cone surface is covered by the Slamet airfall. Erosional processes can diminish and disturb the dimension of the cinder cones, and the result of calculation of volume of all cinder cones is presented in Table 1.

GRAIN SIZE ANALYSIS

Field Characteristics

The term cinder itself is applied to glassy, vesicular ejecta coarser than sand size, ranging up to 2 cm or more in diameter, and the material is light in weight and the particles show glazed, pulled, or freshly broken surfaces that are often iridescent when fresh (Wentworth and McDonald, 1953). They added that some cinders are extremely light, ranging to reticulate, but the more common texture is pumiceous, with irregular, complete vesicles. Material that is mostly 0.5 to 4 mm in diameter and fairly dense is commonly called "black sand"; parts that are coarser and more vesicular are called cinders.

The bombs are vesicular and convolute, consisting of fusiform, breadcrust, and ballistic bombs. The bombs are commonly found intercalated within the layers of airfall, but some of the cinder cones are mainly composed of angular ballistic bombs. These bombs are similar in shape, size, and lithology to the still-intact fractured lava rinds of the breadcrust bombs. It is possible that many of the

blocks are derived from large breadcrust bombs which, when chilled, were fractured and broken apart as they rolled (Heiken, 1978). This process was also observed at Paricutin, Mexico by MacDonald (1972). In cross section, the spherical bombs have a vesiculated core with a great amount of vesicles, ranging from 5 mm to 3 cm in diameter. The vesicles tend to become smaller and denser from the core to the surface. Heiken (1978) also described an accretionary bomb from cinder cone, consisting of an agglomerate core, uniform lava rind, and blocks and bombs impressed into the outer rind surface. The lava rind is dense, has fine vesicles and is commonly cracked by a network of irregular fractures, which usually penetrate the rind. Furthermore, Heiken (1978) described the formation of the accretionary bombs as follows : (1) talus within the crater was mixed with and coated by lava, and (2) the agglomerate, bounded by and coated with lava was ejected to the crater rim where it rolled down the outer slope, picking up debris on molten surfaces, like a rolling snowball. The rolling is indicated by the armoring with talus fragments and the absence of secondary craters, associated with the accretionary bombs.

The interior crater walls of the cinder cones consist of nearly horizontal to outward-dipping layered pyroclastics (ash and bombs). Some bomb-rich layers are cemented by finer-grained cinders or scoria. The vent itself is filled with talus from collapse of the vent walls, and overlain by Slamet airfalls.

The cinder cone deposits on Mount Slamet are light scoriaceous cinders, rounded, mostly 5 to 15 cm in diameter, glassy, and dark grey. Iridescent skin of weathered cinders is a light brown to brownish red intercalation among the fresh cinders. Weathered materials were very pumiceous cinders. The cinders consist of interbedded, graded, grey and brownish red coarse airfall beds averaging from 20 to 40 cm thick (as measured on the Gunung Malang cone), but the layers show indistinct stratifications. Almost all of the beds are normally graded from vesicular lapilli and coarse-grained ash at the base upward to slightly finer-grained gray and brown ash at the top. In exposures on the crater walls, the beds are commonly more than 1 m thick. Some pyroclastic beds in the cinder cones are dominantly composed of bombs: bread crust, fusiform, and ballistic bombs, poorly sorted, poorly stratified, ranging from 1 to 10 cm in

Table 1. The Dimension of Mount Slamet Cinder Cones

No.	Cinder cone's name	Latitude S	Longitude E	Wco (km)	Wcr (km)	Hco (km)	Volume (km ³)
1	Mt. Cilik	7°11'00"	109°12'00"	0.285	0.060	0.061	1.632
2	Mt. Sangin	7°11'12"	109°17'00"	0.430	0.240	0.063	5.882
3	Mt. Kembang	7°11'23"	109°17'09"	0.335	0.090	0.092	3.600
4	Mt. Siremeng	7°11'30"	109°17'00"	0.350	0.175	0.054	2.996
5	Mt. Silempel	7°11'S1"	109°16'44"	0.330	0.055	0.069	2.340
6	Mt. Sarangan	7°11'53"	109°17'00"	0.555	0.290	0.126	0.018
7	Mt. Asuringkuk	7°12'00"	109°17'16"	0.625	0.260	0.113	0.019
8	Mt. Kedunglesung	7°12'16"	109°16'16"	0.560	0.390	0.076	0.014
9	Mt. Kandanggotong	7°12'23"	109°16'52"	0.130	0.040	0.027	1.680
10	Mt. Kondang	7°12'46"	109°17'05"	0.615	0.140	0.106	0.014
11	Mt. Jawar	7°12'46"	109°16'46"	0.500	0.240	0.144	0.016
12	Mt. Sari	7°12'39"	109°16'19"	0.270	0.140	0.058	1.965
13	Mt. Clekatakan	7°12'46"	109°15'44"	0.600	0.205	0.149	0.021
14	Mt. Wanti	7°12'48"	109°15'30"	0.310	0.185	0.127	6.171
15	Mt. Pejagan	7°13'12"	109°17'21"	0.275	0.100	0.055	1.596
16	Mt. Pisang	7°13'30"	109°17'05"	0.430	0.140	0.079	5.565
17	Mt. Lompong	7°13'55"	109°17'16"	0.725	0.155	0.149	0.026
18	Mt. Kaliurip	7°14'05"	109°16'42"	0.390	0.250	0.143	0.012
19	Mt. Tampingan	7°13'49"	109°16'14"	0.650	0.310	0.138	0.026
20	Mt. Dipajaya	7°13'44"	109°16'00"	0.370	0.190	0.055	3.402
21	Mt. Malang	7°13'51"	109°15'39"	0.365	0.170	0.096	5.600
22	Mt. Kaji	7°14'07"	109°16'00"	0.445	0.240	0.159	0.015
23	Mt. Antilang	7°14'19"	109°16'00"	0.370	0.175	0.125	7.689
24	Mt. Tambekor	7°14'25"	109°17'00"	0.425	0.210	0.091	7.536
25	Mt. Sumbul	7°14'49"	109°17'05"	0.350	0.165	0.105	5.589
26	Mt. Pring	7°14'37"	109°16'23"	0.450	0.150	0.122	9.344
27	Mt. Tembelang	7°14'46"	109°16'19"	0.275	0.113	0.125	3.960
28	Mt. Soso	7°14'39"	109°16'10"	0.375	0.160	0.144	8.626
29	Mt. Paingan	7°14'28"	109°15'09"	0.400	0.125	0.133	7.910
30	Mt. Malang	7°15'S8"	109°15'09"	0.475	0.225	0.135	0.013
31	Mt. Rancakele	7°12'S1"	109°20'02"	0.490	0.160	0.137	0.012
32	Mt. Tepus	7°12'28"	109°19'19"	0.370	0.075	0.082	3.762
33	Mt. Malang	7°12'23"	109°19'37"	0.425	0.110	0.118	7.440
34	Mt. Rampak	7°12'14"	109°19'S1"	0.330	0.072	0.079	2.898
35	Mt. Terbang	7°10'44"	109°18'42"	0.750	0.350	0.185	0.045
						Total	0.357

diameter of olivine basalt. The beds of bombs are thick and cemented or interlocked by finer-grained ash materials. Well consolidated layers makes the cinder cone resist to erosion. Juvenile and surface water penetrated the deposits passing through the

pores. The cinder cones are also preserved from erosion, because they are covered by Slamet airfalls. Intensive erosion occurs within the craters, particularly on the crater walls to form bowl-shaped bases.

In some cinder beds at the angle of repose, the

fragments are finer at the base and grade upward to coarser material at the top, giving way again to the finer material of the base of another such layer. This is the reverse of what might result from winnowing of heterogeneous products of a single explosion (Wentworth and MacDonald, 1953). It is possible that the mechanism of explosion produce more finely comminuted fragments at the beginning of a spasm than toward the end. It was also suggested that this effect may due to a progressive accumulation by rolling and sliding, on the premise that coarse material will roll on finer, but not the reverse.

In the cinder cones of Mount Slamet the accessory fragments of pyroxene andesite are often found, that probably indicate that the cinder cones occur over the andesitic rock deposits. The rock fragments are presumably carried up as the cinder cones were building up. In other cases, rock fragments, such as altered sandstone and mudstone, were found mixed with cinders in the farthest cinder cones from the vent, that were built up over the Tertiary rocks.

Shape of the Particles

Volcanic Bombs

Volcanic bombs are fragments of lava that were liquid or plastic at the time of ejection assuming characteristic forms as a result of forces acting during flight (Wentworth and MacDonald, 1953). There is much varieties in form of bombs in Mount Slamet cinder cones, consisting of fusiform (almond-shaped), bread crust (accretionary), and ballistic bombs, and range from less than 5 cm to 50 cm long. Settle (1979) described the fusiform bombs which are typically due to a modification during flight of a blob of lava detached from other lava at both ends. Settle also described the chief factors involved in shaping the bomb are the surface tension, which tends to produce the globosely form, and the fluid drag of surrounding air that tends to cause skin flowage and develops a contrast between the forward and following sides. Settle (1979) stated that "the spiral motion causes the bomb to develop earlike projections on the ends of its axis of rotation". The dominant elements of shape are the continuity of comparable cross section from end to end caused by pulling, the thickening of the middle brought about by surface tension while aloft, and the surface drag and contrast between stoss and lee sides caused by

air resistance and drag while holding a nearly steady orientation during the flight.

Breadcrust bombs that were rarely found in the cinder cones showed shrinkage cracks on their skins, and generally were found in the cinder cones which are close to the vent of Mount Slamet. The bomb is dark grey and quite heavy, ranging from 5 cm to 15 cm with spherical shapes, showing clearly plagioclase and olivine among microlite groundmass. Heiken (1978) distinguished bread crust and accretionary bombs. Accretionary bombs are commonly cracked by a network of irregular fractures which usually penetrate the rind, and characterized by agglomerated cores of densely packed angular lava fragments which are bounded by a small amount of lava matrix. This bomb is also called ropy bomb as a characteristic of Strombolian and Hawaiian activity (Wentworth and MacDonald, 1953).

Ballistic bombs found in Mount Slamet cinder cones light in weight, dark grey of basalt with iridescent dark brown surface. The bombs have large vesicles, particularly in the core, and smaller toward the edges. The rind shows an irregular surface consisting of fine vesicles, or broken vesicles and is qualitatively rough. The largest vesicle is on the order of 1 cm deep; more typical ones are 3 - 5 mm deep

Lapilli and Ash

Two types of particle shapes of lapilli and ash which are recognized in the Slamet cinder cones consist of achneliths and basaltic clasts. The particles are very light in weight and easily broken, ranging from fine-grained ash to lapilli. The term achnelith (from the Greek achne = spray) is applied by Walker (1971) to particles of ash or lapilli grades, up to 32 mm in diameter. Walker also mentioned this particle as pendant-like, spindle-shaped, filamentous, hook-like or banana-shaped. Wentworth and MacDonald (1953) mentioned the particles as Pelee's hair. They occur from the hot up-draft of active fountains which permits spinning of glass during the period of several seconds corresponding to the trajectory of the higher fountains, and the branching and complex forms are probably due to collision and adherence while still plastic.

Particles are generally of equal form and have fracture-bounded surfaces (Walker, 1971). The par-

ticles are found in variable grain sizes of juvenile basaltic fragments, mixed with essential or accessory materials. The vesicles within individual pyroclasts are mostly deformed ovoid, and many adjacent vesicles are linked to form a partly-open network. Minerals within the pyroclasts are olivine and plagioclase phenocrysts and some pyroclasts also contain small tachylite xenoliths within the glass.

Grain Size Characteristics

The causes of variation in grain size parameters of airfall deposits with respect to distance from their source are the result of a great number of variables (Fisher, 1961). Fisher determined that variables such as viscosity, gas content, and explosivity resulted from different magma compositions and these determine the size, shape, and density of fragments, as well as their angle and height of ejection. External variables acting on fragments include air density, pressure, and humidity, as well as the wind velocity, direction, and turbulence. As shown by these studies, the cinder cones are formed by a Strombolian activity and the cone building process is mainly one of ballistic deposition and slumping, with some of the finer-grained tephra carried away by the wind (McGetchin *et al.*, 1974). Studies of the scoria falls on the twelve of the thirty five Mount Slamet cinder cones, indicate that the pyroclastic deposits consist of scoriaceous basalt, as a product of basaltic eruptions comprising layers of limited area extend around the cones.

Walker (1971) observed the pyroclastic products of basaltic eruptions on land which are characterised by fire fountaining or a strombolian activity. These most commonly constitute cones (of scoria, spatter or ash), and the scoria cones resulting from such activity occur in enormous numbers on modern basaltic volcanoes. Self *et al.* (1974) observed the continuation of strombolian type activity of Eldfell, Heimaey, during the first month produced a 200 m high scoria cone and deposited a thick mantle of airfall scoria over the northern half of the island.

To study the grain size characteristics of the two different types of basaltic pyroclastics from the cinder cones and Slamet airfalls, some fourteen samples have been collected for mechanical analysis from several cones and Slamet airfall in the Mount Slamet area. The samples were sieved following

the procedure of Walker and Croasdale (1972) with a set of sieves chosen to have a half ϕ interval and covering the range $\phi = -4$ to $+2.5$ (16 to 0.125 mm). Cumulative curves have been drawn (Figure 11), from which the parameters $Md \phi$ (the median diameter, equals to the ϕ -value at which the cumulative curve crosses the 50 % line) and $\delta\phi$ (the deviation, equals $0.84 \cdot 0.16/2$) have been derived.

The value of $\delta\phi$ for each sample is plotted against $Md \phi$ (Figure 12) separately for the cinder cones and Slamet airfalls. It can be seen that the cinders/scoria composing the cinder cones are on the whole coarser-grained, and generally less poorly sorted, than the Slamet airfalls. The results of twelve cinder cone and two Slamet airfall size-parameter calculations are presented in Table 2. The two Slamet airfall samples are significantly different. The younger Slamet airfall (not plotted in the map) is coarser-grained and better sorted than the older one (Slamet airfall in accompanying geologic map).

Inman (1952) concluded that material carried by agents of transportation are rocks with median diameter of between 0.125 mm and 0.25 mm, will be best sorted. Inman also concluded that as the median increases or decreases from these values, sorting becomes steadily poorer for water-laid sediments as well as for wind blown deposits such as loess. For most strombolian deposits no information is available on wind speed, although the dispersal and grain size characteristics of pyroclastic fall deposits are dependent on, for example, wind strength and direction, the height of eruption column, the style of activity, and the degree of fragmentation of the magma (Self, 1974). Plots of median diameter ($Md \phi$) and sorting coefficient ($\delta\phi$) (Figure 13) illustrate that coarse-grained tephra from the cinder cones becomes more poorly sorted as grain size increase. The histogram of average weight percent for all cinder cone samples against the grain size diameter (ϕ) (Figure 14a) shows a normal distribution, but with a fire tail. In comparison with Slamet airfall (Figure 14b), the cinder cones are significantly different, which presumably indicates the differences of sorting and grain size. Another possibility is the differences of eruption types, where the cinder cones are built by the strombolian activity, and Slamet airfall as a result of the Plinian eruptions. Self (1974) considered that break-up of fragments on landing of scoria falls,

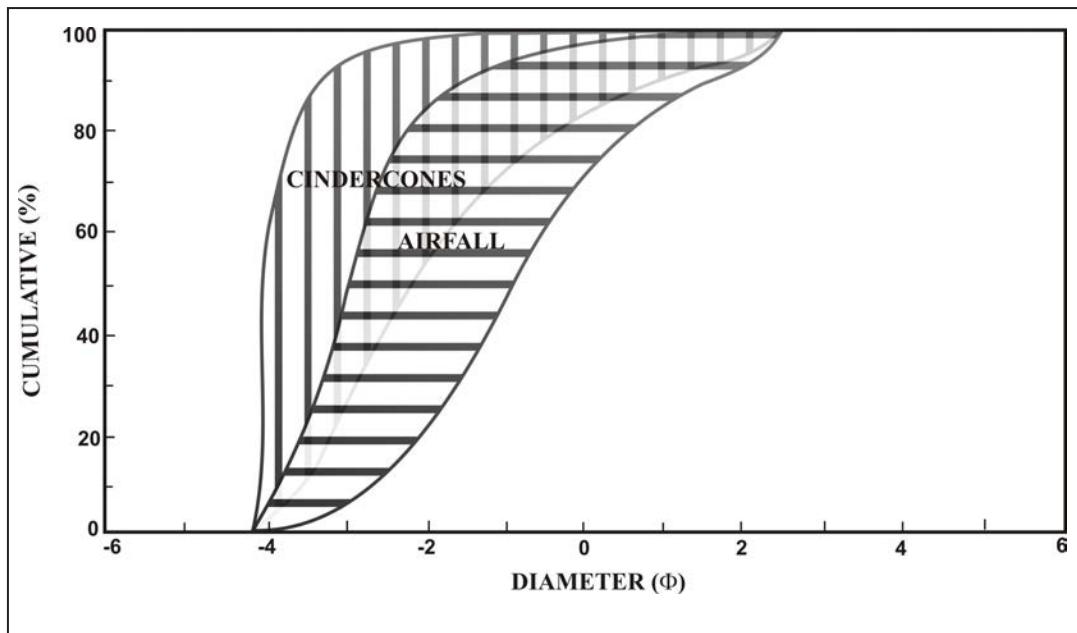


Figure 11. Relationship between the cinder cones and Slamet airfalls.

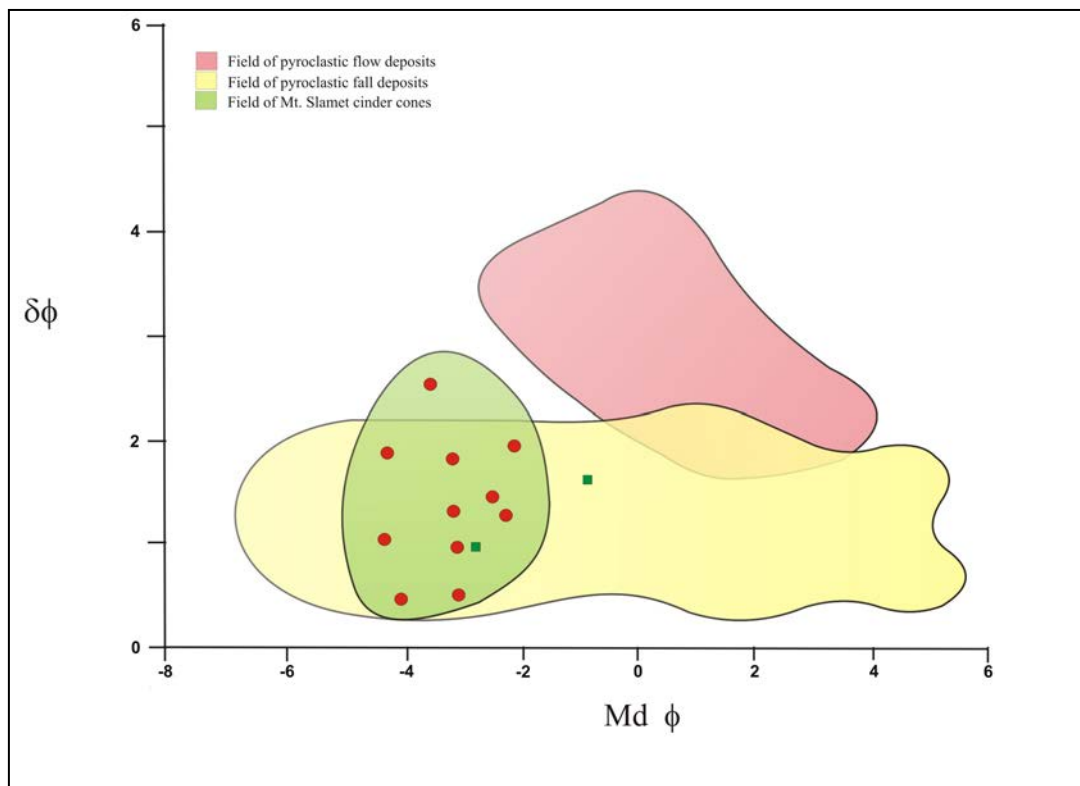


Figure 12. $Md \phi / \delta \phi$ plot used to show the fields of pyroclastic airfall and flow fields (after Walker, 1971), compared to the mount airfalls (green square) and cinder cones (red dots).

and the original air-borne population is coarser and perhaps better sorted than that found on the ground. In addition, Walker (1972) stated that the plinian deposits are generally well-sorted, coarse-grained near source and they show uniformly well-developed down wind sorting.

Table 2. The Grain Size Parameter of the Cinder Cone and Slamet Airfalls

Location	Md ϕ	$\delta\phi$
Mt. Asuringkuk	-3.57	2.50
Mt. Dipajaya	-2.14	1.92
Mt. Tampingan	-4.31	1.02
Mt. Kaji	-3.21	1.78
Mt. Malang	-3.17	1.28
Mt. Tepus	-3.10	0.49
Mt. Rancakele	-3.10	0.94
Mt. Sumbul	-4.29	1.87
Mt. Sarangan	-2.46	1.43
Mt. Kembang	-4.03	0.45
Mt. Terbang	-2.25	1.24
Slamet airfall	-0.79	1.60
Younger Slamet airfall*	-2.76	0.96

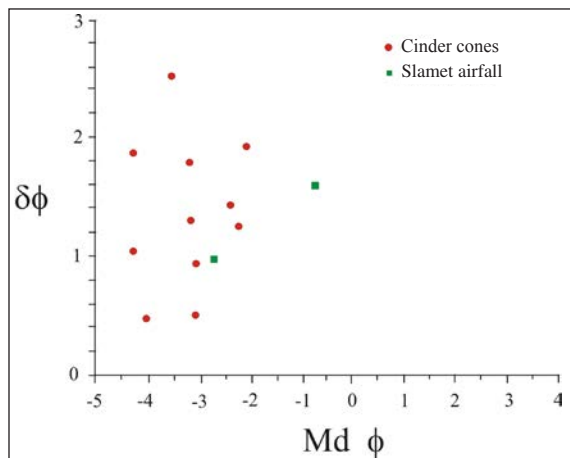


Figure 13. A plot of Md ϕ against $\delta\phi$ for the cinder cone and Slamet airfall deposits.

DISCUSSIONS

The cinder cones on Mount Slamet have a specific distribution just around the east flank of the volcano. Mount Slamet itself is a stratovolcano that

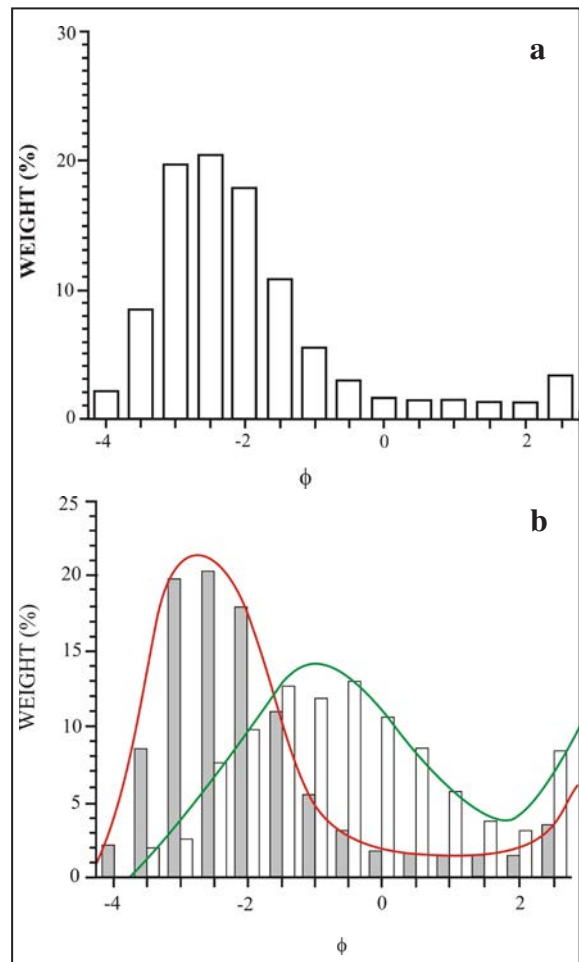


Figure 14. The average grain size distribution for all the cinder cones (a), and a comparison of grain size distribution between the cinder cones and Slamet airfalls (b).

has a stratigraphic record of repeated eruptions from one center, but recently the crater tends to become smaller, and move towards the northwest. In contrast, the cinder cone craters were formed in each cone, with more than one crater in several cinder cones. Comparison of the deposits of twelve cinder cones suggests that there is no significant difference among the cinder cone deposits, and all tephra were emplaced in a dry condition. No evidence of hydro-volcanic eruptions occurs in the cone field. The deposits mainly consist of poorly bedded and poorly sorted vesicular lapilli to bombs. The presence of highly vesicular tephra down to a few millimeters suggests that the large bubbles envisaged to rise alongside vesiculating pyromagma (Blackburn

et al., 1976). On Stromboli, normal degassing was accompanied by 'roar and rush' sounds similar to those accompanying outlet of gas under pressure, and each sound is followed by a puff of gas and, occasionally, ejection of pyroclasts. This behavior is interpreted as the bursting of sizeable bubbles on the lava surface (Blackburn *et al.*, 1976), as has previously been interpreted for lava lakes (MacDonald, 1972). MacDonald also described the strombolian activity as a 'weak to violent ejection of partly fluid blobs' associated with thick lava flows of block lava. According to McGetchin *et al.* (1974) the clots of partly fluid lava and ash are produced when jets of melting materials, accelerated by a gas release, break up into clusters of pyroclasts with mean size ranging from 150 mm to 10 cm. Blackburn *et al.* (1976) presented evidence that large bursting gas bubbles caused the explosive eruption of magma clots at Heimaey, Iceland and Stromboli, Italy.

The tephra from the cinder cones are similar in most respects to that of active eruptions, that is a moderately to poorly sorted lapilli or ash size tephra (Table 2), coarse-grained and highly vesicular. The growth of the cinder cones were controlled by the size and spacing of crustal fractures. The concentric spacing fractures on the east flank of Mount Slamet is probably responsible for the cinder cone construction, but the obvious structures which controlled the eruptive vents are NW-trending strike slip faults that can be observed from either topographic maps and aerial photographs or field observations. McGetchin *et al.* (1974) suggested that the cinder cones grow through four distinct stages: (1) simple cone, with mantle bedding and a low rounded rim, (2) onset of an exterior talus slope, (3) destruction of the original rounded rim by a backward migration of the talus, and (4) outward growth of the talus slope beyond the ballistic limit. The volcanic activity responsible for the construction of a cinder cone field, commonly, represents the most recent phase of volcanism within a particular region, whilst the distribution of the youngest cones within a field reflects the current configuration of subsurface conduits and dikes connecting the regional surface to magma storage reservoirs at depth (Settle, 1979). The direction of these cinder cone alignments coinciding with the relative motion vector of the Eurasian and Indian plates through the Java Island (Hatherton and Dick-

inson, 1969) is consistent with the idea that tectonic stresses control the location of magmatic conduits (Nakamura, 1977).

Morphometric analysis of individual cone field have resulted that variation in cinder cone shape can be correlated with the length of time a cone has been exposed to a particular set of erosive processes (Scott and Trask, 1971; Wood, 1978). This study has shown the average ratio of cone height and cone diameter within a cone field, but it is not directly correlated with the exposure age of the field. Settle (1979) determined a reference line of cone height equals 0.2 cone basal diameter as a characteristic of the initial shape of the cinder cone in Mauna Kea volcanic province prior to erosive degradation. Comparing to Bloomfield *et al.* (1977), a mean cone height/basal diameter ratio for Holocene cones of 0.21 and a mean ratio of cone height/basal diameter ratio of 0.19 for relatively young 'well formed' Pleistocene cones have been determined.

There are two possibilities of the curious dimensions of the cinder cones on Mount Slamet indicated by a mean ratio of 0.25: (1) the cinder cones are relatively young (0.042 Ma), and (2) the cones were preserved from degradation by overlying younger airfall from Mount Slamet activity. The differences in cone shape may result from the more severe weathering environment and heavy rainfall that tend to accelerate the down slope movement of surficial material on the cinder cones.

CONCLUSIONS

Most of the thirty five cinder cones of Mount Slamet lie along the northwest-trending fault system, and are also controlled by radial fractures which may be related to the radial faults just surrounding beyond the study area. The cinder cones occur singly or in a small group ranging from mounds less than 130 m in basal diameter and only several meters high, to hills as much as 750 m across the base and 250 m high, and the presence of most of the cinder cones was due to the strombolian eruption. They generally lie on the Tertiary sediments, and are buried by the Mount Slamet volcanic products, particularly lava flows and pyroclastic airfalls. The majority of the cinder cones are concentrated within latitudes 7°11'00" -

7°16'00" S, and longitudes 109°15'00" - 109°18'00" E, with a local cone density of 1.5 cones/km², with total volume is 0.357 km³.

Morphometric analyses shows all of the cinder cones have a mean ratio of cone height being 0.25 of the cone basal width, which is higher than the Hco = 0.2 Wco reference line. The grain size characteristic of the cinder cone deposits compared to Slamet airfalls generally indicate that the particles are coarser-grained and less poorly sorted. The cinder cones are relatively young with the age of around 42,000 years based on the K-Ar age dating of the scoriae taken from Mount Dipajaya.

Acknowledgments—The authors are greatly indebted to the previous Head of Center of Volcanology and Geological Hazard Mitigation, Dr. A.D. Wirakusumah who has given a chance of the investigation. We are grateful to Professor Dr. Tetsuo Kobayashi for his guidance in the field, and Professor Dr. Adjat Sudradjat who gave authors a support to publish the paper. Thanks to all colleagues who have given the authors assistances and support.

REFERENCES

- Blackburn, E., Wilson, L., and Sparks, R. S. J., 1976. Mechanisms and dynamics of strombolian activity. *Journal of Geological Society of London*, 132, p. 429-440.
- Bloomfield, K., Sanchez Rubio, G., and Wilson, L., 1977. Plinian eruptions of Nevado de Toluca volcano, Mexico, *Geologische Rundschau*, 66, p. 120-146.
- Djuri, M., 1975. *Geologic map of the Purwokerto and Tegal Quadrangles, Java*, scale 1 : 50.000. Geological Survey of Indonesia.
- Eaton, G. P., 1982. The basin and range province: origin and tectonic significance, A Review. *Earth and Planetary Science*, 10, p.409 - 440.
- Fisher, R. V., 1961. Proposed classification of volcanoclastic sediments and rocks. *Geological Society American Bulletin*, 72, p. 1409-1414.
- Hamilton, W., 1979. *Tectonic of the Indonesian region*, Geological Survey Professional Paper, no. 1078.
- Hatherton, T. and Dickinson, W. R., 1969. The relationship between andesitic volcanism and seismicity in Indonesia, the Lesser Antilles, and other island arc. *Journal of Geophysical Research*, 74 (2), p. 5301-53 10.
- Heiken, G., 1978. Characteristics of tephra from cinder cone, Lassen Volcanic National Park, California. *Bulletin of Volcanology*, 41 (2), p. 119-130.
- Inman, D. L., 1952. Measures for describing the size distribution of sediments. *Journal of Sedimentary Petrology*, 22, p. 125-145.
- Katili, J. A., 1969. Large transcurrent faults in Southeast Asia with special reference to Indonesia. *Bulletin of National Institute Geology and Minerals*, 2 (3), p. 21-30.
- Kear, D., 1957. Erosional stages of volcanic cones as indicators of age. *New Zeland Science Technology*, 38-B, p. 671-682.
- MacDonald, G. A., 1972, *Volcanoes*. Englewood Cliffs, New Jersey: Prentice-Hall
- McGetchin, T. R., Settle, M., and Chouet, B.H., 1974. Cinder cone growth modeled after Northeast crater, Mt. Etna, Sisyly. *Journal of Geophysicl Research*, 79, p. 3257-3272.
- McGetchin, T. R. and Settle, M., 1975. Cinder cone separation distances: implications for the depth of formation of grabboic xenoliths. *EOS*, 56, p. 1070.
- Nakamura, K., 1977. Volcanoes as possible indicators of tectonic stress orientation - pricipale and proposal. *Journal of Volcanology and Geothermal Research*, 2, p. 1-16.
- Neumann van Padang, M., 1951, Catalogue of active volcanoes of the world including solfatara fields, part 1, Indonesia. *International Volcanologist Association Italia*, Napoli, 271 pp.
- Pardyanto, L., 1971. *Peta geologi daerah gunung Slamet dan sekitarnya – penafsiran potret udara, skala 1: 100.000*. Direktorat Vulkanologi, unpublisch.
- Porter, S. C., 1972. Distribution, morphology and size frequency of cinder cones on Mauna Kea volcano, Hawaii. *Geological Society of America Bulletin*, 83, p. 3607-3612.
- Scott, D. H. and Trask, N. J., 1971. Geology of the lunar crater volcanic field, Nye County, Nevada. *U. S. Geological Survey Professional Paper*, 599 (1), p. 22.
- Self, S., Sparks, R. S. J., Booth B., and Walker, G. P. L., 1974. The 1973 Heimaey strobolian scoria deposit, Iceland. *Geological Magazine*, 111, p. 539-548.
- Settle, M., 1979. The structure and emplacement of cinder cone fields. *American Journal of Science*, 279, p. 1089-1107.
- Sutawidjaja, I. S., Aswin, D., and Sitorus, K., 1985. *Geologic map of Slamet Volcano, Central Java, scale 1: 50.000*. Volcanological Survey of Indonesia.
- Thorarinnsson, S., 1981. The application of tephrochronology in Iceland. In: Self, S. and Sparks, S. (Eds), *Tephra Studies*, Reidel Publication Co., Dordrecht, p. 109 - 134.
- Tjia, H. D., 1978. Active fault in Indonesia. *Geological Society of Malaysia Bulletin*, 10, p. 73-92.
- Van Bemmelen, R. W., 1949. *The geology of Indonesia and adjacent archipelago*. The Hague: Government Printing Office.
- Verwoerd, W. J. and Chevallier, L., 1987. Contrasting types of surtseyan tuff cones on Marion and Prince Edward islands, southwest Indian Ocean. *Bulletin of Volcanology*, 49, p. 399-417.
- Walker, G. P. L., 1971, Grain size characteristics of pyroclastic

- deposits. *Journal of Geology*, 79, p. 696-714.
- Walker, G. P. L. and Croasdale, R., 1972. Characteristics of some basaltic pyroclastics. *Bulletin of Volcanology*, 35, p. 303-317.
- Wentworth, C. K. and G. A. MacDonald, 1953, Structures and forms of basaltic rocks in Hawaii. *U. S. Geological Survey Bulletin*, 994, 48p.
- Wohletz, K. H. and Sheridan, M. F., 1983. Hydrovolcanic explosions II. Evolution of basaltic tuff rings and tuff cones. *American Journal of Science*, 283, p. 358-413.
- Wood, C. A., 1978. Morphometric evolution of composite volcanoes. *Geophysical Research Letters*, 5, p. 437-439.
- Wood, C. A., 1980. Mophometric evolution of cinder cones. *Journal of Volcanology and Geothermal Research*, 7, p. 387-413.

Makalah diterima : 12 Agustus 2008
Revisi terakhir : 12 Februari 2009